



# Global Biogeochemical Cycles

## RESEARCH ARTICLE

10.1002/2017GB005802

### Key Points:

- Agreement of interannual changes on seasonality of atmospheric CO<sub>2</sub> and NDVI
- Larger seasonality of global vegetation index after 2001
- CMIP5 models were unable to reproduce the seasonality of vegetation index

### Supporting Information:

- Supporting Information S1

### Correspondence to:

W. Yuan,  
yuanwpcn@126.com

### Citation:

Yuan, W., Piao, S., Qin, D., Dong, W., Xia, J., Lin, H., & Chen, M. (2018). Influence of vegetation growth on the enhanced seasonality of atmospheric CO<sub>2</sub>. *Global Biogeochemical Cycles*, 32, 32–41. <https://doi.org/10.1002/2017GB005802>



Received 18 SEP 2017

Accepted 12 DEC 2017

Accepted article online 18 DEC 2017

Published online 9 JAN 2018

## Influence of Vegetation Growth on the Enhanced Seasonality of Atmospheric CO<sub>2</sub>

Wenping Yuan<sup>1,2</sup> , Shilong Piao<sup>3</sup> , Dahe Qin<sup>1</sup>, Wenjie Dong<sup>4</sup>, Jiangzhou Xia<sup>5</sup>, Hui Lin<sup>6,7</sup>, and Min Chen<sup>8,9</sup>

<sup>1</sup>State Key Laboratory of Cryospheric Sciences, Northwest Institute of Eco-Environment and Resources, Chinese Academy of Sciences, Lanzhou, China, <sup>2</sup>Laboratory for Regional Oceanography and Numerical Modeling, Qingdao National Laboratory for Marine Science and Technology, Qingdao, China, <sup>3</sup>College of Urban and Environmental Sciences, Peking University, Beijing, China, <sup>4</sup>School of Atmosphere Science, Sun Yat-Sen University, Guangzhou, China, <sup>5</sup>State Key Laboratory of Earth Surface Processes and Resource Ecology, Beijing Normal University, Beijing, China, <sup>6</sup>Institute of Space and Earth Information Science, The Chinese University of Hong Kong, Hongkong, China, <sup>7</sup>Department of Geography and Resource Management, The Chinese University of Hong Kong, Hongkong, China, <sup>8</sup>Key Laboratory of Virtual Geographic Environment (Nanjing Normal University), Ministry of Education, Nanjing, China, <sup>9</sup>Jiangsu Center for Collaborative Innovation in Geographical Information Resource Development and Application, Nanjing, China

**Abstract** The amplitude of seasonal fluctuations in concentrations of atmospheric CO<sub>2</sub> has increased over recent decades. Model-based studies suggest that this increase could be the result of enhanced vegetation growth during the growing season and ecosystem respiration in the nongrowing season. Here we investigated seasonal changes in vegetation growth derived from satellite-based observations of the normalized difference vegetation index (NDVI) from 1982 to 2013. We found notable agreement between these observations and interannual variations of seasonality of global atmospheric CO<sub>2</sub>, suggesting that terrestrial vegetation growth is the dominant driver of the seasonality of the concentration of atmospheric CO<sub>2</sub>. Specifically, we found that the trend in seasonality of global vegetation growth was not continuous from 1982 to 2013 and that it increased substantially after 2001. In response, the trend of seasonality in the concentration of atmospheric CO<sub>2</sub> stalled from 1982 to 2000 but increased from 2001 onward. This 2001 change in the growth seasonality trend was largely a result of decreased NDVI during spring and winter. CMIP5 models were unable to reproduce this observed seasonality. Our results showed the dominant role played by vegetation growth in determining atmospheric CO<sub>2</sub> seasonality, highlighting the need to improve representation of vegetation growth in current terrestrial models to adequately indicate seasonal changes in the concentration of atmospheric CO<sub>2</sub>.

## 1. Introduction

Ground- and aircraft-based measurements have shown that the peak-to-trough amplitude of the annual fluctuation in atmospheric CO<sub>2</sub> concentration (hereafter CO<sub>2</sub> seasonality) has significantly increased since the 1950s (Graven et al., 2013; Keeling et al., 1996). For example, previous study reports the amplitude of annual CO<sub>2</sub> seasonal cycle increased by 20% in the equator and by 40% in the high latitude (Keeling et al., 1996). Changes in terrestrial carbon cycle are first proposed two decades ago to explain this phenomenon (Keeling et al., 1996). Other studies have consistently arrived at the conclusion that this increase in seasonality strongly correlates with enhanced photosynthesis during the growing season (Forkel et al., 2016; Graven et al., 2013), increased heterotrophic respiration in autumn (Barichivich et al., 2013; Randerson et al., 1997), and increased cropland productivity (Gray et al., 2014; Zeng et al., 2014).

These studies underscore the role of climate-induced changes to terrestrial ecosystems in regulating CO<sub>2</sub> seasonality. All of these studies, however, used model-based methods to investigate the role of vegetation in regulating CO<sub>2</sub> seasonality. Therefore, our understandings on regulations of terrestrial ecosystems to atmospheric CO<sub>2</sub> concentration strongly depend on the model performance. However, a model-data comparison of gross primary productivity, based on the North American Carbon Program (NACP) site-level interim synthesis, shows a large spread of 26 models in both the magnitude and timing of the simulated gross primary product (GPP) seasonal cycle, and these models cannot capture the seasonal pattern of GPP (Schaefer et al., 2012). On average, the models overestimated GPP in spring and fall and underestimated GPP in summer, and the great improvements still are need to reproduce the GPP seasonality by optimizing the response

functions to changing environmental conditions (e.g., low-temperature response function) (Schaefer et al., 2012). Moreover, another study shows that none of all 26 models in the NACP consistently reproduce observed interannual variability of net ecosystem productivity within measurement uncertainty (Keenan et al., 2012). The limited model performance challenges the role of terrestrial ecosystems in regulating atmospheric CO<sub>2</sub> concentration.

Previous studies used a simple method to indicate the seasonality of atmospheric CO<sub>2</sub>, usually using the peak-to-trough amplitude of the annual fluctuation in atmospheric CO<sub>2</sub> concentration (Graven et al., 2013; Keeling et al., 1996). There are only the observations of 2 months with the highest and lowest concentration of atmospheric CO<sub>2</sub> during a year used to indicate the seasonality of atmospheric CO<sub>2</sub>, which ignores the changes at other months. Moreover, almost all studies only used atmospheric CO<sub>2</sub> observations at several sites, which is quite difficult to indicate the global conditions.

In this study, we combine independent satellite-based observations of normalized difference vegetation index (NDVI) and atmospheric CO<sub>2</sub> concentration starting from 1982 to study the relationship between vegetation growth and enhanced seasonality of atmospheric CO<sub>2</sub>. The specific objectives are to (1) examine the interannual variations of seasonality of global atmospheric CO<sub>2</sub> and NDVI and (2) investigate the regulations of vegetation growth on seasonality changes of global atmospheric CO<sub>2</sub>.

## 2. Materials and Methods

### 2.1. Vegetation Index Data Set

We used the newest release of the advanced very high resolution radiometer (AVHRR) NDVI to indicate vegetation growth from 1982 to 2013. The AVHRR is the nonstationary NDVI version 3 data set made available by NASA's Global Inventory Modeling and Monitoring Study third-generation data set (GIMMS-3g) group (Pinzon & Tucker, 2014). This data set is more commonly referred to as NDVI3g, with the suffix 3g referring to the third generation processing applied to correct for orbital drift effects, calibration, viewing geometry, stratospheric volcanic aerosols, and other errors unrelated to vegetation change. NDVI3g contains global NDVI observations at ~8 km spatial resolution and bimonthly temporal resolution, derived from AVHRR channels 1 and 2, corresponding to red (0.58–0.68  $\mu\text{m}$ ) and infrared wavelengths (0.73–1.1  $\mu\text{m}$ ), respectively. Each 15 day data value is the result of maximum value compositing (Holben, 1996), a process that aims to minimize the influence of atmospheric contamination from aerosols and clouds.

### 2.2. Atmospheric CO<sub>2</sub> Concentration Data Set

Observation package data products of long-term monthly observations at 313 air-sampling sites are available over the period 1982–2011 (Cooperative Global Atmospheric Data Integration Project, 2013) in order to calculate CO<sub>2</sub> seasonality (Masarie & Tans, 1995). GLOBALVIEW-CO<sub>2</sub> provides observations at 7 day intervals, and monthly observations are calculated by averaging all available observations in a given month (Cooperative Global Atmospheric Data Integration Project, 2013). This study used the GLOBALVIEW products that are derived using the data extension and integration techniques described by Masarie and Tans (1995), and we did not exclude the filled values. Global mean CO<sub>2</sub> was calculated evenly without any weighting of the individual sites. If missing 7 day data were >20% of total data for an entire year, the value for that year was indicated as missing. For a site to be included in this study it had minimum of 10 year observations. Eventually, 77 sites were included for analyzing the seasonality of atmospheric CO<sub>2</sub> concentration (Figure 1).

### 2.3. Monthly MODIS GPP Data Set

We used MODIS (Moderate Resolution Imaging Spectroradiometer) GPP (gross primary product; MOD17A2), which is monthly global GPP product with 0.05° spatial resolution from 2001 to 2013 (downloaded from [http://files.nts.gov/data/NTSG\\_Products/MOD17/GeoTIFF/Monthly\\_MOD17A2/GeoTIFF\\_0.05degree/](http://files.nts.gov/data/NTSG_Products/MOD17/GeoTIFF/Monthly_MOD17A2/GeoTIFF_0.05degree/)). The seasonality of GPP was calculated in order to examine the role of GPP in regulating atmospheric CO<sub>2</sub> seasonality.

### 2.4. Monthly Fossil-Fuel CO<sub>2</sub> Emission Data Set

The monthly, fossil-fuel CO<sub>2</sub> emission estimates from 1982 to 2011 were derived from a time series of global, regional, and national fossil-fuel CO<sub>2</sub> emissions (Andres et al., 2011; Boden et al., 2015). The data used here used these tabular, national, mass-emission data and distributed them spatially on a 1° of latitude by 1° of

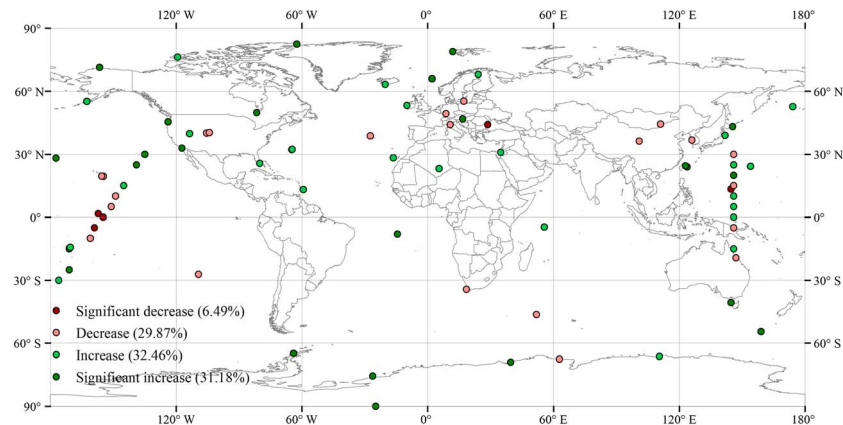


**Figure 1.** Long-term trend on seasonality of atmospheric CO<sub>2</sub> concentration over 77 observation sites. The numbers in the parentheses indicate the site percent with decreased and increased trends.

longitude grid. The within-country spatial distribution was achieved through a fixed population distribution (Andres et al., 1996).

## 2.5. Seasonality Definition and Calculation

We computed a seasonality index based on the NDVI values during the growing season, which is a modification of the previous method (Chave et al., 2010; Zimmerman et al., 2007), as follows:

$$m_x = \frac{1}{n} \sum_{i=0}^{n-1} L^i \cos(d \times i), m_y = \frac{1}{n} \sum_{i=0}^{n-1} L^i \sin(d \times i) \quad (1)$$

$$d = \frac{2 \times \pi}{n} \quad (2)$$

$$SI = \sqrt{m_x^2 + m_y^2} \quad (3)$$

where  $L$  is the NDVI values of  $i$ th bimonthly time and atmospheric CO<sub>2</sub> concentration of  $i$ th month, respectively;  $n$  is the number of observations during one calendar year; and SI is the seasonality index. We tested this method using several dummy biweekly NDVI data sets and found that this index can measure seasonality very well. When NDVI is evenly distributed throughout the year, the index is close to zero; alternatively, the index will increase as seasonality is enhanced (Figure S1a in the supporting information). Moreover, the values of the seasonality index are equal when NDVI values of all months increase with the same magnitude or the NDVI peaks in different months (Figure S1b).

The seasonality index provides a good representation of the seasonal changes of vegetation at the global scale and for various vegetation types. Vegetation seasonality was the highest in high latitude areas and decreased with decreasing latitude (Figures S2 and S3). Moreover, the seasonality index showed substantial differences among vegetation types (Figure S4). The largest value of the seasonality index was found for deciduous needleleaf forests ( $0.1979 \pm 0.03$ ) and the lowest for evergreen broadleaf forests ( $0.0408 \pm 0.02$ ).

## 2.6. Determination of Growing Season

We used surface air temperature ( $T$ , 10 m above the land surface) from the MERRA archive for 1982–2013 at a resolution of  $0.5^\circ$  latitude by  $0.6^\circ$  longitude to determine the growing season (Modern Era Retrospective Analysis for Research and Applications; Global Modeling and Assimilation Office, 2004). The growing season was defined as occurring when the monthly mean air temperature  $> 0^\circ\text{C}$ . This study used the simple method to define the growing season but will not induce risks for results because the analysis was conducted at the monthly scale.

## 2.7. Contribution Analysis

To determine the contribution of monthly NDVI changes to the annual NDVI seasonality, we conducted a simulation experiment based on monthly averaged NDVI, whereby we (1) calculated the mean NDVI values

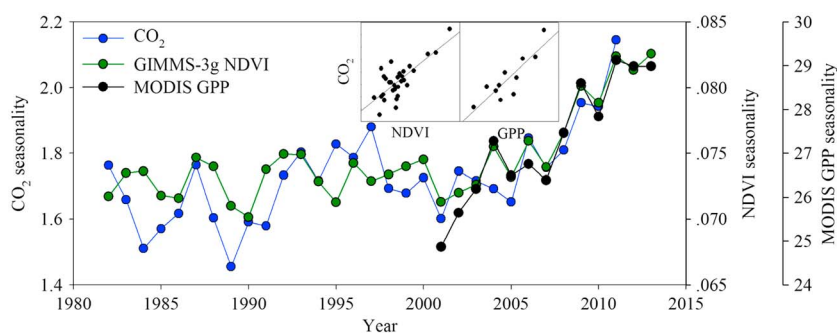


**Figure 2.** Interannual variations in seasonality of global atmospheric CO<sub>2</sub> concentration (blue line), global land surface average GIMMS-3g NDVI (green line) and MODIS GPP (black line). The insets show the correlation of the seasonality index between CO<sub>2</sub> and GIMMS-3g NDVI ( $\text{CO}_2 = 40.01 \times \text{NDVI} - 1.23$ ,  $R^2 = 0.58$ ,  $p < 0.01$ ) and CO<sub>2</sub> and MODIS-GPP ( $\text{CO}_2 = 0.11 \times \text{GPP} - 1.15$ ,  $R^2 = 0.75$ ,  $p < 0.01$ ).

of previous 3 years at  $i$ th month ( $\text{NDVI}_i'$ ) over each grid cell, (2) computed the assumed seasonality index of NDVI ( $\text{SI}_i'$ ) when assumed  $i$ th month NDVI did not have long-term changes based on  $\text{NDVI}_i'$  for all years and actual NDVI values of other months, and (3) calculated the contribution of  $i$ th month NDVI changes to the seasonality index as  $\text{SI}_i = \text{SI} - \text{SI}_i'$ .

### 2.8. Evaluation of Earth System Models for Reproducing Seasonality

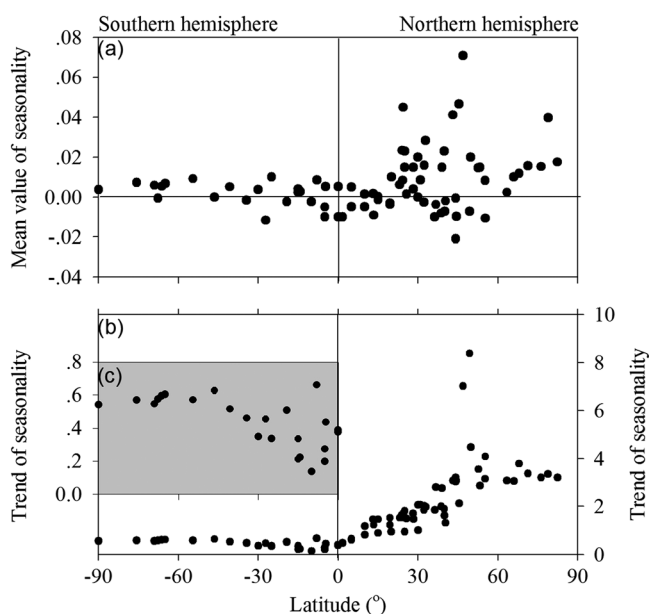
To examine model performance in simulating seasonality of vegetation growth, we compared the satellite-based NDVI and historical simulations of leaf area index (LAI) from a subset of Earth system models (ESMs) currently participating in the fifth phase of the Coupled Model Intercomparison Project (CMIP5). First, we examined if the ESMs can reproduce the seasonal variation of LAI. Mean monthly LAI from 1982 to 2005 was calculated at all pixels using the simulations of 23 ESMs and calculated the correlations (i.e., Pearson coefficient) between monthly LAI simulations and NDVI at all pixels. Second, we calculated the global mean long-term change trends of LAI from 1982 to 2005 for all 12 months and calculated the correlations of monthly trends between LAI simulations and NDVI. Third, we compared interannual variability of NDVI and global averaged LAI seasonality derived from CMIP5 models from 1982 to 2005.

## 3. Results

We calculated trends in the seasonal cycle using monthly mean CO<sub>2</sub> concentration from 77 sites across the globe, each with more than 10 years of observations (see section 2). We found an increasing trend in 49 of the observation sites (24 with a statistically significant increase) (Figure 1), and global mean CO<sub>2</sub> seasonality showed a significant increased trend from 1982 to 2011 (Figure 2). A greater increasing trend of CO<sub>2</sub> seasonality was found at high latitudes (Figure 3).

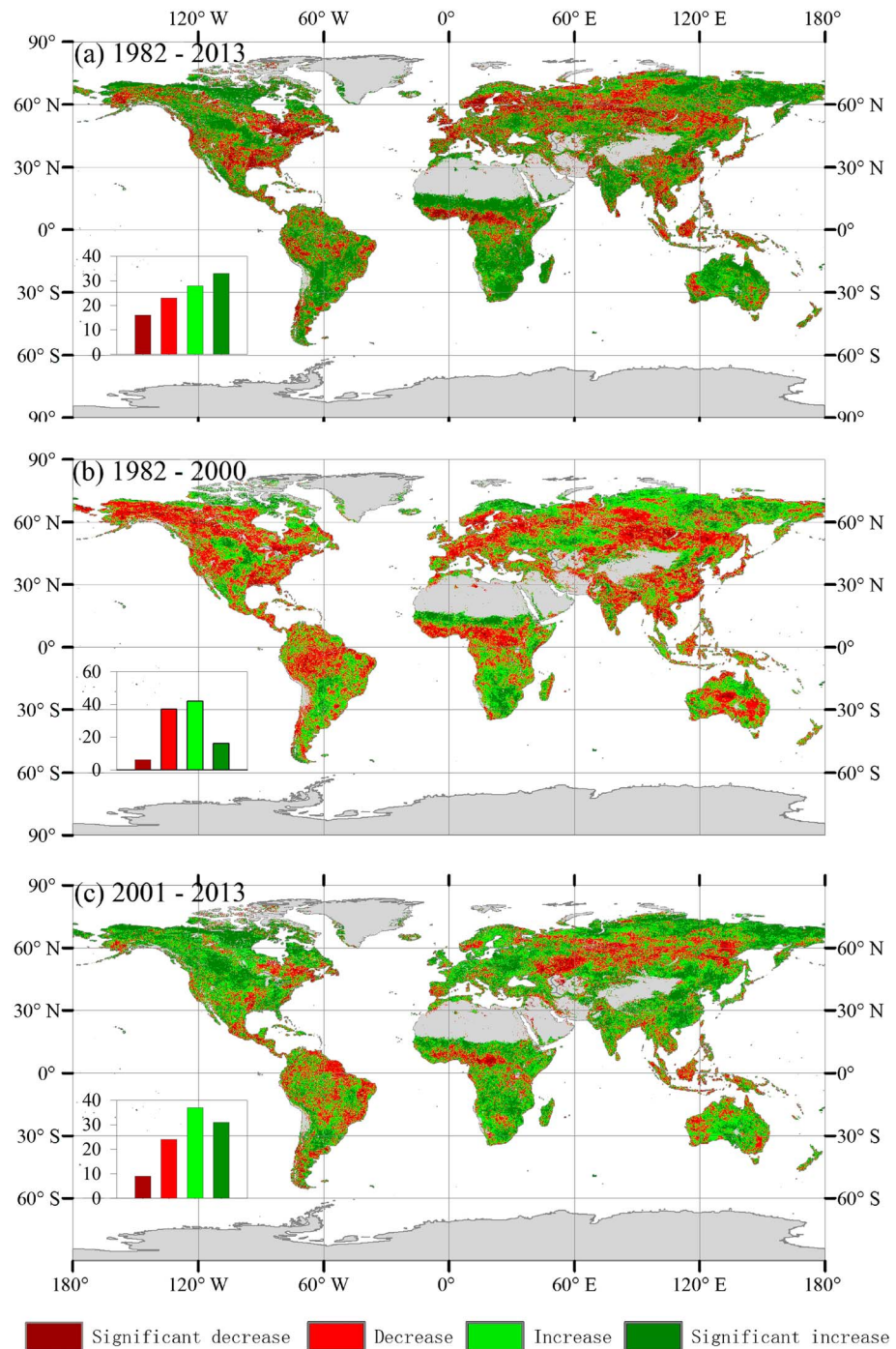
We inferred long-term vegetation growth from a satellite-derived normalized difference vegetation index (NDVI) based on GIMMS-3g and MODIS-GPP product and investigated seasonal changes in vegetation growth and the relationship with atmospheric CO<sub>2</sub> seasonality. The seasonality of global vegetation, indicated by GIMMS-NDVI, has significantly increased during the past 32 years (Figure 2). The seasonality changes in NDVI and GPP are strongly correlated with CO<sub>2</sub> seasonality (Figure 2), which suggests that terrestrial vegetation growth is an important driver of the seasonality in atmospheric CO<sub>2</sub> concentration.

Figure 2 clearly shows that both NDVI and CO<sub>2</sub> seasonality were not temporally homogeneous over the entire 32 years (i.e., from 1982 to 2013): a change of slope is apparent around 2000. A piecewise linear



**Figure 3.** Latitudinal pattern of seasonality in the atmospheric CO<sub>2</sub> concentration over 77 observation sites. (a) Averaged seasonality index; (b) long-term trend of seasonality in the atmospheric CO<sub>2</sub> concentration; (c) local amplification (shadow area) of (Figure 3) to show the trend of seasonality index over the Southern Hemisphere.





**Figure 4.** Global patterns on the trends of NDVI seasonality over the three periods (a) 1982–2013, (b) 1982–2000, and (c) 2001–2013. The insets show the percentage of four changing trends

regression approach quantified the change in trends:  $\text{CO}_2$  seasonality increased slightly from 1982 to 2000 ( $y = 0.009x - 16.66$ ,  $R^2 = 0.21$ ,  $p < 0.05$ ) but increased more strongly from 2001 ( $y = 0.04x - 81.41$ ,  $R^2 = 0.76$ ,  $p < 0.01$ ) (Figures 2 and S5). Similarly, vegetation growth as measured by NDVI clearly showed two distinct periods with a stronger trend after 2000 (Figures 2 and S5). The seasonality spatially averaged over the globe does not significantly change from 1982 to 2000, and there are 16% areas that show a significant increase in seasonality (Figure 4b). During the period 2001–2013, NDVI seasonality significantly

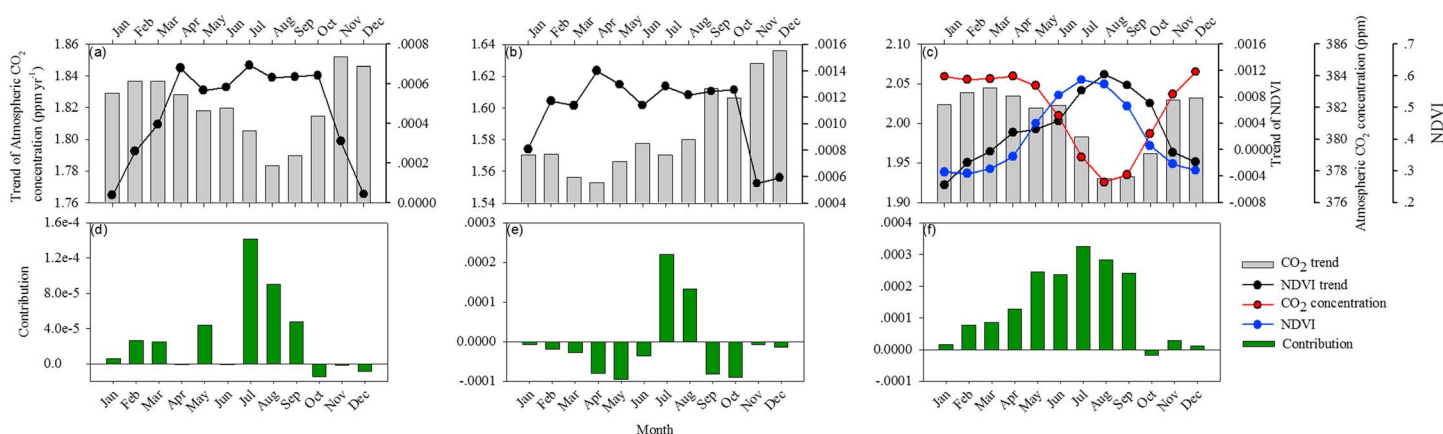


**Figure 5.** Monthly trends of atmospheric CO<sub>2</sub> concentration (gray bars) and NDVI (black lines) during (a) 1982–2013, (b) 1982–2000, and (c) 2001–2013. The red line at Figure 5c indicates the averaged seasonal variation of atmospheric CO<sub>2</sub> concentration from 1982 to 2013. (d–f) Monthly contribution of NDVI changes to NDVI seasonality.

increased with an increasing trend occurring over most of the global land surface (68%; 31% with a significant increase) (Figure 4c).

For each of the three periods investigated (1982–2013, 1982–2000, and 2001–2013), the annual growth rate of global mean NDVI over 12 months negatively correlated with the changes in concentrations of atmospheric CO<sub>2</sub> (Figures 5a–5c and S6). In general, larger increases in the months with higher CO<sub>2</sub> concentration will enhance CO<sub>2</sub> seasonality. Over the period 1982 to 2000, CO<sub>2</sub> concentration in October, November, and December showed the largest increases, and this acted to enhance CO<sub>2</sub> seasonality (Figure 5b). However, the magnitude of increases in CO<sub>2</sub> concentration from January to May, another period with high CO<sub>2</sub> concentrations, was very slight, and this acted to depress CO<sub>2</sub> seasonality (Figure 5b). In contrast, from 2001 to 2013, increases of CO<sub>2</sub> during January to April and October to December were higher than those during June to September (Figure 5c), and both acted to enhance CO<sub>2</sub> seasonality. The monthly trends of NDVI were negatively correlated with the trends of global atmospheric CO<sub>2</sub> growth (Figure S6), highlighting the strong regulation of vegetation activity to changes in concentrations of atmospheric CO<sub>2</sub>.

The difference in NDVI seasonality changes before and after 2000 was strongly determined by the heterogeneous changes of various months. We quantified the monthly contributions to changes of NDVI seasonality (see method). Over the period of 1982–2000, only the NDVI changes in July and August contributed positively to NDVI seasonality, and the NDVI changes of all other months decreased NDVI seasonality (Figure 5e). In contrast, from 2001 to 2013, NDVI changes in most months increased NDVI seasonality (Figure 5f) and showed larger effects than those from 1982 to 2000. Globally, there was a large total area where NDVI experienced lower increases or decreases over 2001–2013 compared to that of 1982–2000 (Figure 6). In particular, MAM (March, April, and May) (61%) and DJF (December, January, and February) (63%) had large areas with lower NDVI increases, and JJA (June, July, and August) (55%) and SON (September, October, and November) (54%) had slightly larger areas of NDVI stagnation (Figure 6).

#### 4. Discussion

This study showed the influence of vegetation growth on the enhanced seasonality of atmospheric CO<sub>2</sub>, which supports previous studies that the terrestrial ecosystem plays an important role in regulating seasonal changes of atmospheric CO<sub>2</sub> (Barichivich et al., 2013; Forkel et al., 2016; Graven et al., 2013; Randerson et al., 1997). Burning of biomass from wildfires and fossil fuels are two important sources of emissions, which represent forcing trends in the atmospheric CO<sub>2</sub> concentration seasonal cycle. Our analysis shows a very weak correlation between CO<sub>2</sub> seasonality and fossil fuel emissions (Figure S7). This finding is consistent with a previous study demonstrating the limited contribution of fossil fuel emissions in comparison with that produced by the terrestrial ecosystem seasonal cycle. In the Northern Hemisphere, for example, the contribution of fossil fuels to CO<sub>2</sub> seasonality ranges from 5% to 17% (Randerson et al., 1997). Moreover, the contribution

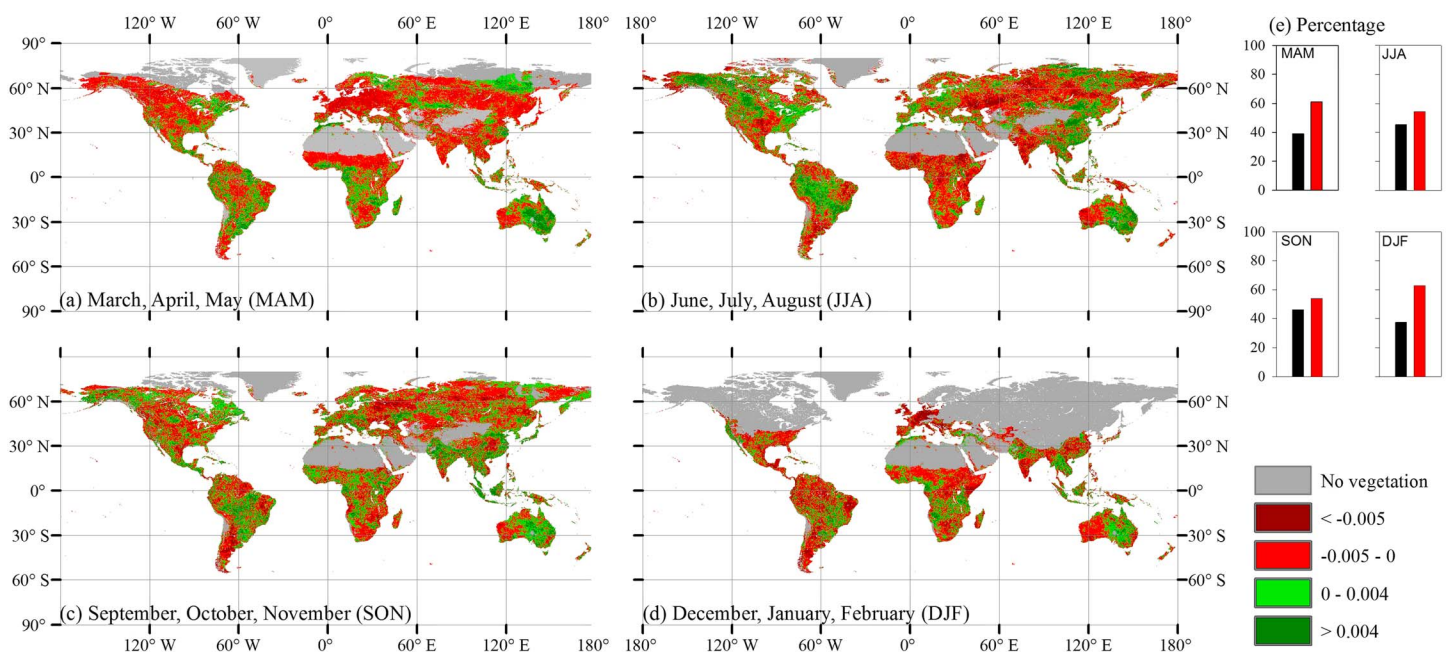


**Figure 6.** Differences in NDVI trends between 2001–2013 and 1982–2000. (a) For March, April, and May. (b) For June, July, and August. (c) For September, October, and November. (d) For December, January, and February. (e) The black bars indicate the global mean percentage of the increased trend and the red bars of the decreased trend of 2001–2013 compared to those of 1982–2000.

of fossil fuels to trends in the seasonal cycle at high-latitude stations in the Northern Hemisphere appeared to decrease during the 1980s as emission rates from high-latitude regions of the Northern Hemisphere stabilized (Randerson et al., 1997). In the Southern Hemisphere, CO<sub>2</sub> seasonality showed increased sensitivity to changes in fossil fuel emissions, but the contributions were still less than 25% (Randerson et al., 1997). Because of the lack of global data on emissions from biomass burning before the 1990s, we did not investigate its impact on atmospheric CO<sub>2</sub> seasonality. However, previous study found that the contribution of biomass burning to the seasonal cycle ranges from 1% to 4% for stations in the Northern Hemisphere (Randerson et al., 1997). In the Southern Hemisphere the contribution of biomass burning to the seasonal cycle is significantly greater than that in the north but is still less than 20%.

This study showed substantial spatial differences in seasonal changes in NDVI over the different latitude bands (Figure S8n). Over the Southern Hemisphere, the increases in NDVI seasonality from 1982 to 2013 were found in all areas (Figure S8n) as a result of larger increases in NDVI occurring in the months with high NDVI values (Figures S8i–S8m). The increases of NDVI seasonality also occurred over the northern high latitudes. This result is quite different from that of a previous study that reported, for the northern latitudes, temperature increases are most pronounced in spring and autumn, and the increases of NDVI during these seasons decrease seasonality (Xu et al., 2013). Moreover, our study calculated seasonality of vegetation growth based on all months during the growing season, and this comprehensively indicated seasonality. However, our results indicated that the largest increases in vegetation growth occur in the summer (Figures S8e–S8i), which enhances vegetation seasonality. Our results showed that the extended growing season and the profound climate warming that occurs during the winter and spring do not reduce vegetation growth seasonality but enhance the seasonality resulting from larger growth increases during the summer.

Other lines of evidence also support the finding that the increase in vegetation growth during the 1980s and 1990s may have stalled or even reversed during the 2000s over Eurasia (Piao et al., 2011), East Asia (Park & Sohn, 2010; Yuan et al., 2014), North America (Wang et al., 2011), and the Southern Hemisphere (Zhao & Running, 2010) (Figure 6). Numerous studies have been conducted to investigate the major causes behind vegetation browning during 2000s, and the factors potentially influencing vegetation growth in different regions and seasons are complex and varied (Park & Sohn, 2010; Yuan et al., 2016; Zhao & Running, 2010). Previous studies highlighted that the increasing water stresses should be the major cause for hindering

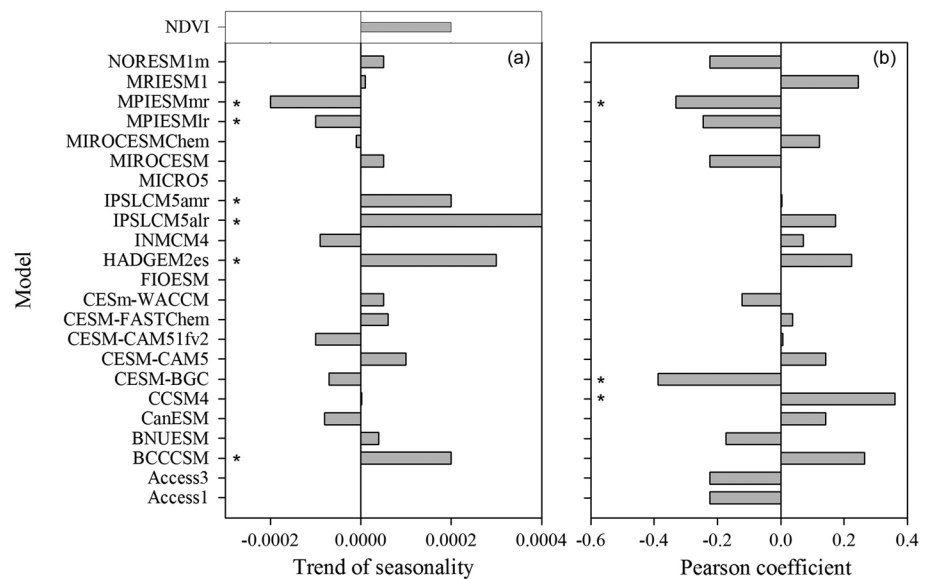


**Figure 7.** Comparison on interannual variability of NDVI and global averaged LAI seasonality derived from CMIP5 models from 1982 to 2005. (a) Long-term trend of NDVI and LAI seasonality; (b) Pearson correlation coefficients of seasonality between simulated LAI and NDVI. \*Significance at the level  $p < 0.05$ .

vegetation growth in the temperate and boreal Eurasia during 2000s (Park & Sohn, 2010; Piao et al., 2011). In the Eurasia, both spring and summer NDVI significantly increased during 1980s and 1990s, but then decreased from 1998, particularly summer NDVI, which may be related to the significant decrease in summer precipitation (Piao et al., 2011). In addition, temperature changes also played an important role in determining vegetation growth in North America and Siberia. In the northwestern region of North American, for example, spring temperature increased until the early 1990s and stalled or decreased afterward. In response, spring and summer vegetation greening trend, which was evident in this region during the 1980s, stalled or reversed since late 1990s (Wang et al., 2011).

To examine model performance in simulating seasonality of vegetation growth, we compared the historical simulations of a subset of terrestrial ecosystem models currently participating in the fifth phase of the Coupled Model Intercomparison Project (CMIP5). The seasonality of simulated vegetation growth varied strongly between models, with changing trends ranging from  $-0.0002$  to  $0.004$  (Figure 7a). There was only one model (namely CCSM4) with both significant and positive correlations between vegetation growth seasonality, as given by LAI (leaf area index) simulations, and satellite-based observations (Figure 7b). Our results highlight the important implications of regulation of atmospheric  $\text{CO}_2$  seasonality by vegetation growth, but the current ecosystem models fail to reproduce this response—a gap in their performance that needs to be filled, if they are to adequately assess the role of vegetation growth in the global carbon cycle.

In addition, we examined the model performance for indicating seasonal differences and long-term change trends of LAI, and both of them jointly determined the change trends of LAI seasonality. The results showed that none of models can indicate well for both of LAI seasonal differences and long-term change trends (Figures S10 and S11). Low model performance largely resulted from inappropriate carbon allocation, turnover time, and phenology simulations. The recent studies compared simulated carbon allocation of net primary production to leaf with global observed allocation fraction, and the results showed substantial differences in the simulated allocations compared with observations over all forest types (Xia et al., 2015; Xia et al., 2017). Moreover, numerous studies reported large uncertainties of leaf turnover time in the current ecosystem models (Friend et al., 2014). For example, Zhang et al. (2016) indicated that the default leaf longevities in LPJ significantly differed from observations for four major forest types—especially, observed leaf longevity of boreal needleleaf forest (6.5 years) was more than 3 times the default model value (2 years). In addition, the simulations on plant phenology phases largely determined model performance for LAI (Xia et al., 2015). Some modeling experiments provide opportunity for analyzing the impacts of phenology on



LAI simulations by prescribing phenology from satellite data (Huntzinger et al., 2013; Sitch et al., 2015). Future research is needed to identify the uncertainty in estimating LAI using these model comparison and experiment data sets.

This study highlights that vegetation growth dominates the changes of atmospheric CO<sub>2</sub> seasonality (Figure 2). However, it should be noticed that ecosystem respiration also plays an important role in regulating CO<sub>2</sub> seasonality (Gray et al., 2014). Figure 3 showed the larger increased trends of CO<sub>2</sub> seasonality at high latitudes; however, the seasonality of vegetation growth did not show the similar latitudinal pattern (Figure S8). Ecosystem respiration potentially contributed the latitudinal increases of CO<sub>2</sub> seasonality. The magnitude of rising air temperature at high latitudes was larger than other regions, and especially the largest rising temperature occurred at winter (IPCC, 2013). Therefore, ecosystem respiration would be simulated jointly impacting by rising temperature and large soil organic carbon content at high latitudes (Celis et al., 2017; Commene et al., 2017). However, current ecosystem models poorly reproduce the seasonal changes of carbon fluxes including vegetation production and ecosystem respiration (Keenan et al., 2012), which limits our understanding on roles of ecosystem respiration to atmospheric CO<sub>2</sub> seasonality. It is imperative to improve model algorithms to adequately assess the impacts of terrestrial carbon cycle on the atmospheric CO<sub>2</sub> concentration.

## 5. Conclusion

This study investigated the regulations of vegetation growth to atmospheric CO<sub>2</sub> seasonality. The results implied that terrestrial vegetation growth dominates the changes of seasonality of atmospheric CO<sub>2</sub>. Especially, the seasonality of global vegetation growth stalled from 1982 to 2000 but substantially increased after 2001. As a consequence, atmospheric CO<sub>2</sub> seasonality did not continuously change and that it increased largely from 2001 onward. In addition, our results showed the poor ability of current terrestrial models to reproducing seasonal changes in the vegetation growth. In general, this study represented the dominant role of vegetation growth in determining atmospheric CO<sub>2</sub> seasonality.

## Acknowledgments

This study was supported by the National Key Basic Research Program of China (2016YFA0602701 and 2015CB954103), Key Project of Chinese Academy of Sciences (CAS) (KJZD-EW-G03-04), the National Science Foundation for Excellent Young Scholars of China (41322005), and One Hundred Person Project of CAS and PAPD (164320H116). All data sets used in this study are available and can be downloaded from relevant websites that have been provided in the manuscript.

## References

- Andres, R. J., Gregg, J. S., Losey, L., Marland, G., & Boden, T. A. (2011). Monthly, global emissions of carbon dioxide from fossil fuel consumption. *Tellus*, 63B, 309–327.
- Andres, R. J., Marland, G., Fung, I., & Matthews, E. (1996). A 1° × 1° distribution of carbon dioxide emissions from fossil fuel consumption and cement manufacture, 1950–1990. *Global Biogeochemical Cycles*, 10(3), 419–429. <https://doi.org/10.1029/96GB01523>
- Barichivich, J., Briffa, K. R., Myneni, R. B., Osborn, T. J., Melvin, T. M., Ciais, P., ... Tucker, C. (2013). Large-scale variations in the vegetation growing season and annual cycle of atmospheric CO<sub>2</sub> at high northern latitudes from 1950 to 2011. *Global Change Biology*, 19(10), 3167–3183. <https://doi.org/10.1111/gcb.12283>
- Boden, T. A., Marland, G., & Andres, R. J. (2015). *Global, regional, and national fossil-fuel CO<sub>2</sub> emissions. Carbon Dioxide Information Analysis Center*. Oak Ridge, TN: Oak Ridge National Laboratory, U.S. Department of Energy. [https://doi.org/10.3334/CDIAC/00001\\_V2015](https://doi.org/10.3334/CDIAC/00001_V2015)
- Celis, G., Mauritz, M., Bracho, R., Salmon, V. G., Webb, E. E., Hutchings, J., ... Schuur, E. A. G. (2017). Tundra is a consistent source of CO<sub>2</sub> at a site with progressive permafrost thaw during 6 years of chamber and eddy covariance measurements. *Journal of Geophysical Research: Biogeosciences*, 122, 1471–1485. <https://doi.org/10.1002/2016JG003671>
- Chave, J., Navarrete, D., Almeida, S., Álvarez, E., Aragão, L. E. O. C., Bonal, D., ... Malhi, Y. (2010). Regional and seasonal patterns of litterfall in tropical South America. *Biogeosciences*, 7(1), 43–55. <https://doi.org/10.5194/bg-7-43-2010>
- Commene, R., Lindaas, J., Benmergui, J., Luus, K. A., Chang, R. Y. W., Daube, B. C., ... Wofsy, S. C. (2017). Carbon dioxide sources from Alaska driven by increasing early winter respiration from Arctic tundra. *Proceedings of the National Academy of Sciences of the United States of America*, 114(21), 5361–5366. <https://doi.org/10.1073/pnas.1618567114>
- Cooperative Global Atmospheric Data Integration Project (2013). Multi-laboratory compilation of synchronized and gap-filled atmospheric carbon dioxide records for the period 1979–2012 (obspack\_co2\_1\_GLOBALVIEW-CO2\_2013\_v1.0.4\_2013-12-23). Compiled by NOAA Global Monitoring Division: Boulder, Colorado, U.S.A. Data product accessed at <https://doi.org/10.3334/OBSPACK/1002>.
- Forkel, M., Carvalhais, N., Rodenbeck, C., Keeling, R., Heimann, M., Thonicke, K., ... Reichstein, M. (2016). Enhanced seasonal CO<sub>2</sub> exchange caused by amplified plant productivity in northern ecosystems. *Science*, 351(6274), 696–699. <https://doi.org/10.1126/science.aac4971>
- Friend, A. D., Lucht, W. L., Rademacher, T. T., Keribin, R., Betts, R., Cadule, P., ... Woodward, F. I. (2014). Carbon residence time dominates uncertainty in terrestrial vegetation responses to future climate and atmospheric CO<sub>2</sub>. *Proceedings of the National Academy of Sciences of the United States of America*, 111, 3280–3285.
- Global Modeling and Assimilation Office (2004). File specification for GEOSDAS gridded output version 5.3, report. Greenbelt, Md: NASA Goddard Space Flight Cent.
- Graven, H. D., Keeling, R. F., Piper, S. C., Patra, P. K., Stephens, B. B., Wofsy, S. C., ... Bent, J. D. (2013). Enhanced seasonal exchange of CO<sub>2</sub> by northern ecosystems since 1960. *Science*, 341(6150), 1085–1089. <https://doi.org/10.1126/science.1239207>
- Gray, J. M., Frolking, S., Kort, E. A., Ray, D. K., Kucharik, C. J., Ramankutty, N., & Friedl, M. A. (2014). Direct human influence on atmospheric CO<sub>2</sub> seasonality from increased cropland productivity. *Nature*, 515(7527), 398–401. <https://doi.org/10.1038/nature13957>
- Holben, B. N. (1996). Characteristics of maximum-value composite images from temporal AVHRR data. *International Journal of Remote Sensing*, 7, 1417–1434.

- Huntzinger, D. N., Schwalm, C., Michalak, A. M., Schaefer, K., King, A. W., Wei, Y., ... Zhu, Q. (2013). The North American Carbon Program (NACP) Multi-Scale Synthesis and Terrestrial Model Intercomparison Project (MSTMIP): Part I—Overview and experimental design. *Geoscientific Model Development*, 6(6), 2121–2133. <https://doi.org/10.5194/gmd-6-2121-2013>
- IPCC (2013). Climate Change 2013: The Physical Science Basis. Contribution of Working Group I to the Fifth Assessment Report of the Intergovernmental Panel on Climate Change. In T. F. Stocker, et al. (Eds.). Cambridge, UK and New York: Cambridge University Press.
- Keeling, C., Chin, J., & Whorf, T. (1996). Increased activity of northern vegetation inferred from atmospheric CO<sub>2</sub> measurements. *Nature*, 382(6587), 146–149. <https://doi.org/10.1038/382146a0>
- Keenan, T. F., Baker, I., Barr, A., Ciais, P., Davis, K., Dietze, M., ... Richardson, A. D. (2012). Terrestrial biosphere model performance for inter-annual variability of land-atmosphere CO<sub>2</sub> exchange. *Global Change Biology*, 18(6), 1971–1987. <https://doi.org/10.1111/j.1365-2486.2012.02678.x>
- Masarie, K. A., & Tans, P. P. (1995). Extension and integration of atmospheric carbon dioxide data into a globally consistent measurement record. *Journal of Geophysical Research*, 100(D6), 11,593–11,610. <https://doi.org/10.1029/95JD00859>
- Park, H. S., & Sohn, B. J. (2010). Recent trends in changes of vegetation over East Asia coupled with temperature and rainfall variations. *Journal of Geophysical Research*, 115, D14101. <https://doi.org/10.1029/2009JD012752>
- Piao, S. L., Wang, X., Ciais, P., Zhu, B., Wang, T., & Liu, J. (2011). Changes in satellite-derived vegetation growth trend in temperate and boreal Eurasia from 1982 to 2006. *Global Change Biology*, 17(10), 3228–3239. <https://doi.org/10.1111/j.1365-2486.2011.02419.x>
- Pinzon, J. E., & Tucker, C. J. (2014). A non-stationary 1981–2012 AVHRR NDVI3g time series. *Remote Sensing*, 6(8), 6929–6960. <https://doi.org/10.3390/rs6086929>
- Randerson, J. T., Thompson, M. V., Conway, T. J., Fung, I. Y., & Field, C. B. (1997). The contribution of terrestrial sources and sinks to trends in the seasonal cycle of atmospheric carbon dioxide. *Global Biogeochemical Cycles*, 11(4), 535–560. <https://doi.org/10.1029/97GB02268>
- Schaefer, K., Schwalm, C. R., Williams, C., Arain, M. A., Barr, A., Chen, J. M., ... Zhou, X. (2012). A model-data comparison of gross primary productivity: Results from the North American Carbon Program site synthesis. *Journal of Geophysical Research*, 117, G03010. <https://doi.org/10.1029/2012JG001960>
- Sitch, S., Friedlingstein, P., Gruber, N., Jones, S. D., Murray-Tortarolo, G., Ahlström, A., ... Myneni, R. (2015). Recent trends and drivers of regional sources and sinks of carbon dioxide. *Biogeosciences*, 12(3), 653–679. <https://doi.org/10.5194/bg-12-653-2015>
- Wang, X. H., Piao, S., Ciais, P., Li, J., Friedlingstein, P., Koven, C., & Chen, A. (2011). Spring temperature change and its implication in the change of vegetation growth in North America from 1982 to 2006. *Proceedings of the National Academy of Sciences of the United States of America*, 108(4), 1240–1245. <https://doi.org/10.1073/pnas.1014425108>
- Xia, J. Z., Chen, Y., Liang, S. L., Liu, D., & Yuan, W. P. (2015). Global simulations of carbon allocation coefficients for deciduous vegetation types. *Tellus (B)*, 67(1), 28,016. <https://doi.org/10.3402/tellusb.v67.28016>
- Xia, J. Z., Yuan, W. P., Wang, Y. P., & Zhang, Q. G. (2017). Adaptive Carbon Allocation by Plants Enhances the Terrestrial Carbon Sink. *Scientific Reports*, 7, 3341. <https://doi.org/10.1038/s41598-017-03574-3>
- Xu, L., Myneni, R. B., Chapin, F. S. III, Callaghan, T. V., Pinzon, J. E., Tucker, C. J., ... Stroeve, J. C. (2013). Temperature and vegetation seasonality diminishment over northern lands. *Nature Climate Change*, 3, 581–586.
- Yuan, W. P., Cai, W., Chen, Y., Liu, S., Dong, W., Zhang, H., ... Zhou, G. (2016). Severe summer heatwave and drought strongly reduced carbon uptake in southern China. *Scientific Reports*, 6(1), 18,813. <https://doi.org/10.1038/srep18813>
- Yuan, W. P., Liu, D., Dong, W., Liu, S., Zhou, G., Yu, G., ... Zhao, L. (2014). Multiyear precipitation reduction strongly decreases carbon uptake over northern China. *Journal of Geophysical Research: Biogeosciences*, 119, 881–896. <https://doi.org/10.1002/2014JG002608>
- Zeng, N., Zhao, F., Collatz, G. J., Kalnay, E., Salawitch, R. J., West, T. O., & Guanter, L. (2014). Agricultural green revolution as a driver of increasing atmospheric CO<sub>2</sub> seasonal amplitude. *Nature*, 515(7527), 394–397. <https://doi.org/10.1038/nature13893>
- Zhao, M. S., & Running, S. W. (2010). Drought-induced reduction in global terrestrial net primary production from 2000 through 2009. *Science*, 329(5994), 940–943. <https://doi.org/10.1126/science.1192666>
- Zhang, H. C., Liu, D., Dong, W. J., Cai, W. W., & Yuan, W. P. (2016). Accurate representation of leaf longevity is important for simulating ecosystem carbon cycle. *Basic and Applied Ecology*, 17, 396–407.
- Zimmerman, J. K., Wright, S. J., Calderón, O., Pagan, M. A., & Paton, S. (2007). Flowering and fruiting phenologies of seasonal and aseasonal neotropical forests: The role of annual changes in irradiance. *Journal of Tropical Ecology*, 23(02), 231–251. <https://doi.org/10.1017/S0266467406003890>